Received: 6 June 2023 | Revised: 30 July 2023 | Accepted: 20 August 2023

DOI: 10.1111/ejss.13417

RESEARCH ARTICLE

European Journal of Soil Science WILEY

Temperature and soil moisture change microbial allocation of pesticide-derived carbon

Johannes Wirsching[1] | **Luciana Chavez Rodriguez**[2,3] | **Franziska Ditterich**[1] | **Holger Pagel**[2] | **Rushan He**[1,2] | **Marie Uksa**[4] | **Christian Zwiener**[5] | **Ellen Kandeler**[1] | **Christian Poll**[1]

[1]Soil Biology Department, Institute of Soil Science and Land Evaluation, University of Hohenheim, Stuttgart, Germany

[2]Biogeophysics Department, Institute of Soil Science and Land Evaluation, University of Hohenheim, Stuttgart, Germany

[3]Department of Ecology and Evolutionary Biology, University of California Irvine, Irvine, California, USA

[4]Department of Environmental Microbiology, Helmholtz Centre for Environmental Research GMBH-UFZ, Leipzig, Germany

[5]Institute of Applied Geoscience, Department of Environmental Analytical Chemistry, University of Tübingen, Tübingen, Germany

Correspondence
Johannes Wirsching, Soil Biology Department, Institute of Soil Science and Land Evaluation, University of Hohenheim, Emil-Wolff-Str. 27, 70599 Stuttgart, Germany.
Email: johannes.wirsching@uni-hohenheim.de

Funding information
Collaborative Research Center 1253 CAMPOS (DFG), Grant/Award Number: 1253/12017; Deutsche Forschungsgemeinschaft; DFG Priority Program 2322 "Soil System"; Ellrichshausen Foundation; Research Training Group "Integrated Hydrosystem modeling", Grant/Award Number: RTG 1829

Abstract

Temperature and soil moisture are known to control pesticide mineralization. Half-life times (DT_{50}) derived from pesticide mineralization curves generally indicate longer residence times at low soil temperature and moisture but do not consider potential changes in the microbial allocation of pesticide-derived carbon (C). We aimed to determine carbon use efficiency (*CUE*, formation of new biomass relative to total C uptake) to better understand microbial utilization of pesticide-derived C under different environmental conditions and to support the conventional description of degradation dynamics based on mineralization. We performed a microcosm experiment at two MCPA (2-methyl-4-chlorophenoxyacetic acid) concentrations (1 and 20 mg kg^{-1}) and defined 20°C/pF 1.8 as optimal and 10°C/pF 3.5 as limiting environmental conditions. After 4 weeks, 70% of the initially applied MCPA was mineralized under optimal conditions but MCPA mineralization reached less than 25% under limiting conditions. However, under limiting conditions, an increase in *CUE* was observed, indicating a shift towards anabolic utilization of MCPA-derived C. In this case, increased C assimilation implied C storage or the formation of precursor compounds to support resistance mechanisms, rather than actual growth since we did not find an increase in the *tfdA* gene relevant to MCPA degradation. We were able to confirm the assumption that under limiting conditions, C assimilation increases relative to mineralization and that C redistribution, may serve as an explanation for the difference between mineralization and MCPA dissipation-derived degradation dynamics. In addition, by introducing *CUE* to the temperature- and moisture-dependent degradation of pesticides, we can capture the underlying microbial constraints and adaptive mechanisms to changing environmental conditions.

KEYWORDS
anabolism, carbon use efficiency, catabolism, effect of soil moisture and temperature, gene-centric process model, MCPA biodegradation

1 | INTRODUCTION

Pesticide residues in European arable soils have become an environmental threat of great concern (Silva et al., 2019). Microbial degradation is the most important process to reduce this pesticide contamination (Schwarz et al., 2022), whereby degradation rates depend primarily on soil temperature (Helweg, 1993). How accessible the pesticide residues are to microbial degradation is influenced by the soil moisture content (Schroll et al., 2006). A very common method to determine the degradation rate and residence time under various temperature and soil moisture conditions is to evaluate the mineralization of $^{13}C/^{14}C$-labelled pesticides (Bouseba et al., 2009; Dörfler et al., 1996; Helweg, 1987; Helweg, 1993; Schroll et al., 2006). However, assessing pesticide degradation and pesticide persistence based on mineralization curves alone does not address how microbial C-allocation of pesticide-derived C changes in response to soil temperature and moisture. Shifts in microbial C allocation alter microbial carbon use efficiency (*CUE*), defined as the ratio of newly synthesized biomass C to total C uptake. A low *CUE* is characterized by a relatively high mineralization rate, while a high *CUE* is an indication of enhanced growth and potential C stabilization in soils (Manzoni et al., 2012). Considering that pesticides are linked to the carbon (C) cycle when pesticides serve as the sole source of C and energy (Pagel et al., 2016), *CUE* can be used to evaluate the fate of pesticides under changing environmental conditions and support the interpretation of pesticide degradation based solely on mineralization curves, as *CUE* allows us to predict whether more C will be respired or utilized to form new biomass and eventually stored as biomass residues (bioNER) in the soil (Muskus et al., 2019). Consequently, increased *CUE* may indicate that mineralization-derived half-lives anticipate longer residence times that do not match the dynamics of actual pesticide decline.

Generally, *CUE* increases with declining temperature during soil organic matter degradation, indicating an increase in the relative allocation of assimilated C to growth (Allison et al., 2010). For specialized pesticide degraders, this has not yet been proven. Even though a temperature increase from 10 to 20°C has been shown to accelerate pesticide mineralization (Choi et al., 1988; Helweg, 1987; Muskus et al., 2020; Thirunarayanan et al., 1985), lower temperatures do not always lead to a significant decrease in degradation. Lower temperatures may instead lead to a C redistribution within the microbial cell, where less CO_2 is emitted, as more C is used to maintain existing biomass (Allison et al., 2010). Muskus et al. (2019) found that a temperature drop from 20 to 10°C resulted in less mineralization of labelled $^{13}C_3$, ^{15}N-glyphosate, but promoted the formation of ^{13}C non-extractable residues (NER; proteins + other remaining bioNER + sorbed and sequestered compounds (xenoNER)). However, because bioNERs were only determined after the death of the microorganisms, information on C dynamics during pesticide turnover was lost. Soil moisture is one of the most important parameters regulating biological activities in soils (Schroll et al., 2006) and can influence pesticide fate in soils by facilitating the contact between degraders and pesticides due to diffusion and mass flow (Jury et al., 1987). Increasing water content within a soil water potential range of −1.5 to −0.015 MPa (Moyano et al., 2013; Schroll et al., 2006) intensifies the degradation of pesticides (Griffin, 1981; Helweg, 1987). For example, 2-methyl-4-chlorophenoxyacetic acid (MCPA) persists 10 times longer in dry soils than in moist soils (Audus, 1952) due to the moisture-sensitive exponential growth of microbes (Helweg, 1987). As aridity increases, microorganisms must invest more energy (Parr et al., 1981) in overcoming the suction tension that holds the water in the soil (Griffin, 1969). As energy requirements in drier soils increase, it is conceivable that the way microbes allocate C will have a profound impact on pesticide mineralization rates. Specifically, drought-tolerant microbes invest heavily in the formation of extracellular enzymes to maintain C uptake for the synthesis of stress response compounds such as osmolytes, cryoprotectants, and chaperones (Schimel et al., 2007) to stabilize cell pressure (Manzoni et al., 2014). This would imply that pesticide degradation still occurs under low soil moisture conditions, but it is not reflected in the ^{14}C mineralization which is no longer proportional to the dynamic of the overall degradation processes. This mechanism has already been demonstrated for soil C turnover by Zeglin et al. (2013), in which soil C sequestration potential was higher under dry conditions.

The degradation rate also depends on the initial pesticide concentration (Karanasios et al., 2012; Schoen &

Highlights

- Limiting environmental conditions (low soil moisture and temperature) reduce MCPA mineralization.
- MCPA-derived C utilization shifted towards an anabolic metabolism under limiting conditions.
- A higher CUE could explain the differences between mineralization and MCPA residue-derived degradation dynamics.

Winterlin, 1987; Wirsching et al., 2020). Pesticide degradation at low concentrations usually follows first-order kinetics and is often astonishingly fast (Fomsgaard & Kristensen, 1999; Helweg et al., 1998). In contrast, pesticide degradation at high concentrations is initially limited by the number of microorganisms, leading to a lag phase and the typical S-shaped mineralization curve. The onset of microbial growth is decisive for effective degradation here (Wirsching et al., 2020). With respect to C-allocation, in a previous study (Wirsching et al., 2020), we demonstrated that the predominantly catabolic use of MCPA at concentrations ≤ 1 mg kg^{-1} shifted towards a gradually increasing anabolic metabolism at concentrations ≥ 5 mg kg^{-1}. If initial pesticide concentration determines C use by microbial pesticide degraders, the impacts of temperature and moisture on C allocation may also depend on pesticide concentration.

In this study, we aimed to link pesticide degradation to *CUE*. *CUE* as a metric to describe pesticide-derived C allocation could explain differences in the dynamics of pesticide mineralization and dissipation under changing environmental conditions. We used ^{14}C-labelled MCPA as a model compound since it is a weakly adsorbing pesticide (Patzko, 2009) that is readily soluble in water (Fredslund et al., 2008) and highly biodegradable (Oh et al., 1995). Moreover, the functional genes involved in MCPA degradation have been well characterized (Nicolaisen et al., 2008). We hypothesized that (i) reducing soil temperature and moisture increases the anabolic utilization of MCPA and that this (ii) could explain the differences in mineralization and dissipation dynamics. We also expected that (iii) the effect size would be more pronounced at higher initial MCPA concentrations. To test these hypotheses, we determined the temporal relationship between mineralization ($^{14}CO_2$) and biomass formation ($^{14}C_{mic}$, i.e., *CUE*), and measured alterations in microbial degradation activity (*tfdA* mRNA) and MCPA-degrading genetic potential (*tfdA* DNA). To complement the experimentally determined *CUE*, we calibrated a gene-centric model using the experimental data (mineralization, *tfdA* mRNA, and *tfdA*). Based on the calibrated model, we predicted two model-based *CUE*s to interpret the pesticide-derived C use of MCPA-specific degraders.

2 | MATERIALS AND METHODS

2.1 | Soil origin and sampling

The study site was in the central region of the Ammer catchment in southwest Germany (48°33′24.664″, 8°52′31.259″). Soil samples were taken in March 2019 from an Ap-horizon (0–30 cm) of a silty Luvisol (World Reference Basis for Soil Resources). According to farmers' records of their cultivation and spraying programs dating back to 1990, MCPA had never been applied to the agricultural field. The main pesticides applied were chloridazone and metamitron. After sampling, the soil was sieved (2 mm), homogenized, and stored at −20°C (−80°C for mRNA samples) to prevent further biological reactions. The main characteristics of the soil are shown in Table 1.

2.2 | Experimental design

The experimental setup consisted of two soil temperatures (10 and 20°C), two soil moisture levels (pF 1.8 and 3.5), and two concentration treatments of ^{14}C ring-labelled MCPA (1 and 20 mg kg^{-1} dry weight) plus one control treatment without MPCA application. In this study, we defined 10°C, pF 3.5, and the lower MCPA concentrations as limiting conditions, and 20°C, pF 1.8, and the higher MCPA concentration as optimal conditions for microbial degradation. We chose concentrations based on Wirsching et al. (2020) because first-order degradation is very rapid at 1 mg kg^{-1} and microbial growth does not occur until 20 mg kg^{-1}. Additionally, 20 mg kg^{-1} represents typical applications of MCPA in the field. A set of microcosms with all treatment combinations consisted of 36 samples (2 soil moisture levels × 2 soil temperature levels × 3 MCPA concentrations (including the control) × 3 replicates). Four of these sets were prepared, yielding in total of 144 microcosms (Figure S1). MCPA solution was uniformly applied to adjust gravimetric soil water content to 39.6% (pF 1.8) and 29.1% (pF 3.5). Subsequently, after thoroughly mixing the soil with the MCPA solution, cylinders (diameter = 5.6 cm, height = 4 cm) were filled with 100 g of soil and compacted to a bulk density of 1.2 g cm^{-3} (height of the soil core was 3 cm). In three of these sets (108 microcosms), ^{14}C-ring labelled MCPA with an activity of 15 kBq (99% purity, specific activity 50–60 mCi $mmol^{-1}$; BIOTREND Chemikalien GmbH, Germany) was applied. One set was sacrificed at each of three-time points (5, 15, and 28 days, sampling schedule Table S2) to quantify ^{14}C incorporation into microbial biomass ($^{14}C_{mic}$). Time points were selected according to the evolution of the $^{14}CO_2$ mineralization curve, i.e., in the initial lag phase (no $^{14}CO_2$ evolution), in the exponential degradation phase (maximum $^{14}CO_2$ evolution), and in the final saturation phase (renewed decrease in $^{14}CO_2$ evolution). In the last sacrificed set, $^{14}CO_2$-respiration was measured every second day. In the fourth set (36 microcosms) only unlabeled MCPA (analytical MCPA purity 99.2%, Sigma-Aldrich, Germany) was applied. A series of subsamples (on every second

TABLE 1 Chemical and physical soil properties.

Soil horizon	Depth	pH	C_{org}	Nitrogen	Phosphate	Sand	Silt	Clay
Ap	[cm]	[$CaCl_2$]	[mg g^{-1}]	[mg g^{-1}]	[mg g^{-1}]	[%]	[%]	[%]
	0–30	6.48	18.4	2.1	1.038	2.26	72.04	23.8

day) was taken and stored at −20°C for MCPA quantification and at −80°C for RNA/DNA co-extraction (RNA stability can only be guaranteed at −80°C) until the analysis.

2.3 | MCPA dissipation analysis

MCPA was extracted from 2 g of soil dissolved in a suspension of 10 mL methanol/water (1:1) as described by Pagel et al. (2016). MCPA was quantified by HPLC-MS/MS analysis (tandem mass spectrometry; Agilent 6490 iFunnel Triple Quadrupole (QqQ), Waldbronn-Germany). The recovery of total MCPA from soil samples was greater than 98% with a detection limit of 13 mg kg^{-1} (detailed information in the Supplement).

2.4 | MCPA mineralization ($^{14}CO_2$)

To determine the MCPA-derived $^{14}CO_2$ respiration, an aliquot of 1 mL was taken every second day from a trap containing 2 mL 1 M NaOH set up in the microcosm. It was then mixed with 4 mL of scintillation liquid (Rotiszint Eco Plus, Carl Roth GmbH + Co. KG) in a 5 mL scintillation vial (LDPE). The decay rate in becquerels (Bq) was measured using a scintillation counter (Wallac 1411, Liquid Scintillation Counter, USA, detailed information in the Supplement). The half-life times (DT_{50MIN}) derived from the cumulative mineralization curves were calculated from the estimated parameters of equations 1 and 2 (see also Duo-Sen and Shui-Ming (1987) and Wirsching et al. (2020)):

$$C = C_0 \cdot \left(1 - \frac{1}{(1-f_k)\cdot e^{k_1 \cdot t} + f_k}\right) \quad (1)$$

$$DT_{50MIN} = \frac{1}{k_1} \cdot \ln\left[\frac{1}{1-f_k} + 1\right] \quad (2)$$

where C is the MCPA-derived $^{14}CO_2$ (% of MCPA initially applied), C_0 is the total mineralizable MCPA that was not immediately incorporated into the microbial biomass or bound to the soil organic matter after application (% of MCPA initially applied), k_1 (d^{-1}) is the rate constant of MCPA degradation per day, and and f_k is a dimensionless parameter, where the range of f_k is constrained as $0 \leq f_k < 1$ (Wirsching et al., 2020).

2.5 | Microbial biomass (C_{mic})

Microbial biomass was estimated using the chloroform fumigation extraction method (CFE) developed by Vance et al. (1987), adapted by Poll et al. (2010) for an additional ^{14}C determination. To obtain the ^{14}C content in C_{mic}, 1 mL of the CFE supernatant was mixed with 4 mL scintillation liquid (Rotiszint Eco Plus, Carl Roth GmbH+Co. KG) in a 5 mL scintillation vial (LDPE). Subsequently, the decay rate in Bq was determined using a scintillation counter (Wallac 1411, Liquid Scintillation Counter, USA). Calculation of the incorporated ^{14}C was performed as described for the C_{mic} content in the Supplement.

2.6 | MCPA degrader abundance and activity

2.6.1 | DNA/RNA co-extraction

For RNA and DNA extraction, 2 g frozen soil was weighed into 15 mL bead-beating tubes and extracted using the RNAeasy PowerSoil Total RNA Kit for soil (Qiagen, Germany) and the RNAeasy PowerSoil DNA Elution Kit (Qiagen, Germany) in a co-extraction method following the manufacturer's protocol. Before using the RNA samples for Real-Time quantitative PCR (qPCR), the possible remaining DNA in the RNA samples was digested using the TURBO DNA-free™ Kit (Invitrogen, Thermo Fisher Scientific, Germany, Table S3).

2.6.2 | Real-time quantitative PCR

For gene quantification (bacterial 16S rRNA and functional genes), qPCR assays were applied using an ABI Prism 7500 Fast system (Applied Biosystems, Germany) with SYBR Green detection. The primer and qPCR conditions used are listed in Table S5. Each SYBR Green reaction contained 7.5 µL of Power SYBR® Green PCR master mix (Applied Biosystems, Germany),

0.75.µL of each primer (5 µM), 0.375 µL of T4gp32 (MP Biomedicals, Germany), 3.625 µL water and 2 µL diluted template DNA or cDNA (3 ng μL^{-1}) for functional genes (*tfdA* and *cadA*). For 16S rRNA, 1 µL diluted template DNA or cDNA (3 ng μL^{-1}) and 4.625 µL of water were used. For quantification, standard plasmid DNA was used with a dilution series from 10^8 to 10^1 copies μL^{-1} according to Ditterich et al. (2013). *CadA* showed no response to MCPA addition and was therefore not considered during the study.

2.7 | Gene-centric modelling of MCPA biodegradation

We used a recently developed modelling approach Chavez Rodriguez et al. (2020) to simulate MCPA mineralization (C_P [mmol g^{-1}]), *tfdA* genes and transcripts [copies g^{-1}], and CUE. The original modelling approach was extended to account for constitutive gene expression and to include a temperature response function as follows:

1. We assumed gene expression to be in quasi-steady state described by the Hill function, including constitutive gene expression that is potentially important at low concentrations

$$\widehat{mRNA} = f_T \cdot \left(\frac{\left(C_P^L\right)^{n_H}}{\left(C_P^L\right)^{n_H} + \left(K_G\right)^{n_H}} + \frac{\alpha}{f_T} \right) \quad (3)$$

where f_T represents the number of transcripts per gene, n_H [−] and K_G [mmol cm^{-3}] are the Hill exponent and Hill constant respectively, α is the constitutive gene expression coefficient set to $1.2 \cdot 10^{-5}$ transcripts per gene (Leveau et al., 1999), and C_P^L [mmol cm^{-3}] is the solution phase concentration of MCPA.

2. We used the temperature response function $f_R(T)$ from Sierra et al. (2015), which influences microbial growth, but also the decay rate, exogenous and endogenous maintenance rates, and decay rate of NER, and is defined as follows:

$$f_R(T) = (Q_{10})^{\left(\frac{T-10C}{10C}\right)} \quad (4)$$

where Q_{10} [−] is the temperature function constant, and T is the temperature in °C.

The full model description, process formulations, and model equations can be found in the Appendix S1: Section 1.7. Model parameter ranges are found in Table S6.

2.7.1 | Model calibration

We performed a hierarchical model calibration using the parameter ranges from Table S6. Model calibration was achieved by minimizing the sum of squared error (*SSE*) with the optimization algorithm Simulated Annealing from MATLAB:

$$SSE = \sum_{i=1}^{n} \frac{\left(y^i_{measured} - y^i_{simulated}\right)^2}{\sigma_i^2} \quad (5)$$

where $y_{measured}$ is the mean value of the i^{th} observation, $y_{simulated}$ is the corresponding i^{th} simulated value, and σ^2 is the standard deviation of the corresponding observations.

The hierarchy of parameter groups was formed by assuming: (i) different bacterial subpopulations under the two different initial concentrations of MCPA (C), (ii) possible physiological and morphological bacterial changes under different moisture levels (W) that were not well captured by moisture functions found in the literature, and (iii) specific soil-dependent parameters (S). Thus, parameters for calibration were grouped according to the proposed hierarchy (Table S6).

Model outputs corresponding to the measured data for model calibration are the following:

$$\text{Mineralization } [\%] = \frac{^{14}CO_2 \cdot 100\%}{^{14}C^0_{MCPA}} \quad (6)$$

$$\text{Genes } \left[\text{copies } g^{-1}\right] = \frac{C_B}{f_1} \quad (7)$$

$$\text{Transcripts } \left[\text{copies } g^{-1}\right] = \frac{\widehat{mRNA} \cdot C_B}{f_1} \quad (8)$$

$$\text{Residual MCPA } \left[\text{mg } kg^{-1}\right] = C_P^L \cdot \frac{\theta}{\rho} + K_P \cdot \left(C_P^L\right)^{n_P} \quad (9)$$

$$\text{DT}_{50\text{RES}} \left[d^{-1}\right] = Time\left[\left(\text{Residual MCPA} = 0.5 \cdot C^0_{MCPA}\right)\right] \quad (10)$$

where f_1 [mmol $gene^{-1}$] is the conversion factor cell to C (Table S6). Incorporation of ^{14}C into the microbial biomass (C_{mic}) as well as CUE were not used for model calibration.

We complemented our model calibration with a local sensitivity analysis of our parameter fits through the sensitivity coefficient (Ingalls, 2008; Zi, 2011), identifiability score (Malwade et al., 2017; Yao et al., 2003), and error (Malwade et al., 2017) of estimated parameters.

2.8 | Carbon use efficiency

We derived *CUE* both experimentally and with two model-based CUE_S:

1. CUE_M: experiment-based *CUE* used for labelled substances (Geyer et al., 2016)

$$CUE_M = \frac{^{14}C_{mic}}{^{14}C_{mic} + ^{14}CO_2} \quad (11)$$

where: $^{14}C_{mic}$ is the C uptake in microbial biomass, and $^{14}CO_2$ is the mineralized MCPA-derived C.

2. CUE_E: environmental model-based *CUE* adapted from Geyer et al. (2016).

$$CUE_E = \frac{C_B^{14}}{C_B^{14} + ^{14}CO_2} \quad (12)$$

3. CUE_C: community model-based *CUE* adapted from Geyer et al. (2016) and Manzoni et al. (2018).

$$CUE_C = 1 - \frac{r^{14}_{respiration} + r^{14}_{m-endogenous} + r^{14}_{m-exogenous} + r^{NER}_{decay}}{r^{14}_{respiration} + r^{14}_{growth} + r^{14}_{m-exogenous}} \quad (13)$$

2.9 | Statistical analysis

A linear model with mixed effects as part of the "nlme" package using the lme function (Pinheiro et al., 2020) implemented in R version 3.5.2 was applied, specifying concentration, soil moisture, temperature, and their interactions as fixed effects, with microcosms as random effects. Response variables were ^{14}C mineralization rate, ^{14}C uptake, CUE, *tfdA* gene expression, and *tfdA* abundance. Model assumptions from ANOVA were visually confirmed by residual diagnostic plots (Kozak & Piepho, 2018). For the specification of contrasts between the influencing factors relevant to the verification of our hypothesis, a post-hoc comparison was conducted using the package "emmeans" (Lenth et al., 2020). With this package, the estimated marginal means were calculated, and interaction plots were made by using the "emmip" function to display the interactions between the variables soil moisture, temperature, and concentration. The influences of the variables were compared pairwise with the Tukey method, and the standard error (SE) and *p*-value for each result were simultaneously computed.

3 | RESULTS AND DISCUSSION

3.1 | Enhanced MCPA mineralization under elevated temperature and moisture

Pesticide degradation studies often fail to consider the possibility that the efficiency of microbial C utilization can shift in response to environmental factors (Allison et al., 2010; Manzoni et al., 2012). Our study, therefore, analysed microbial utilization of the pesticide MCPA in response to limiting (10°C/pF 3.5) and optimal (20°C/pF 1.8) environmental conditions. In addition to estimating the mineralization of ^{14}C-labelled MCPA and the dynamics of specific degraders, we calculated the *CUE* to evaluate microbial C allocation to catabolic and anabolic processes. Our analyses were complemented by a mechanistic gene-based model fitted to the experimental data (Table S8).

Maximum microbial MCPA mineralization among treatments was determined by accumulated $^{14}CO_2$ production at the end of the incubation period (Figure 1a–d). Under optimal soil conditions (20°C, pF 1.8) and 20 mg kg^{-1}, nearly 70% of the initially applied ^{14}C-labelled MCPA was mineralized. Under limiting conditions (10°C, pF 3.5) and 1 mg kg^{-1}, mineralization was significantly reduced and peaked at only 23%. These results were confirmed by our model simulations, which accurately depicted the measured mineralization (Figure 1a–d).

3.1.1 | Temperature response

As a single factor, a temperature increase from 10 to 20°C resulted in an increase in $^{14}CO_2$ mineralization of 10.5% ($F_{1,16} = 73.9$, $p < 0.01$). However, the effect was significantly more pronounced at high MCPA concentrations (+17.7%) than at low MCPA concentrations (+3.4%, $F_{1,16} = 35.2$, $p < 0.001$; Figure 1a–d). Comparable temperature-dependent increases in mineralization were demonstrated in studies by Nowak et al. (2020) and Muskus et al. (2020) for glyphosate, Helweg (1993) for mecoprop (MCPP), and Bouseba et al. (2009) for 2,4-D. These increases in ^{14}C mineralization appeared to be independent of the chemical properties and associated behaviours of those pesticides in soils. In our experiment, an explanation could be found in the temperature sensitivity of the enzyme-catalysed reactions of MCPA degradation, which are associated with inherent kinetic properties (intrinsic temperature sensitivity) and a concentration-dependent response of mineralization rates to temperature (apparent temperature sensitivity; Davidson & Janssens, 2006).

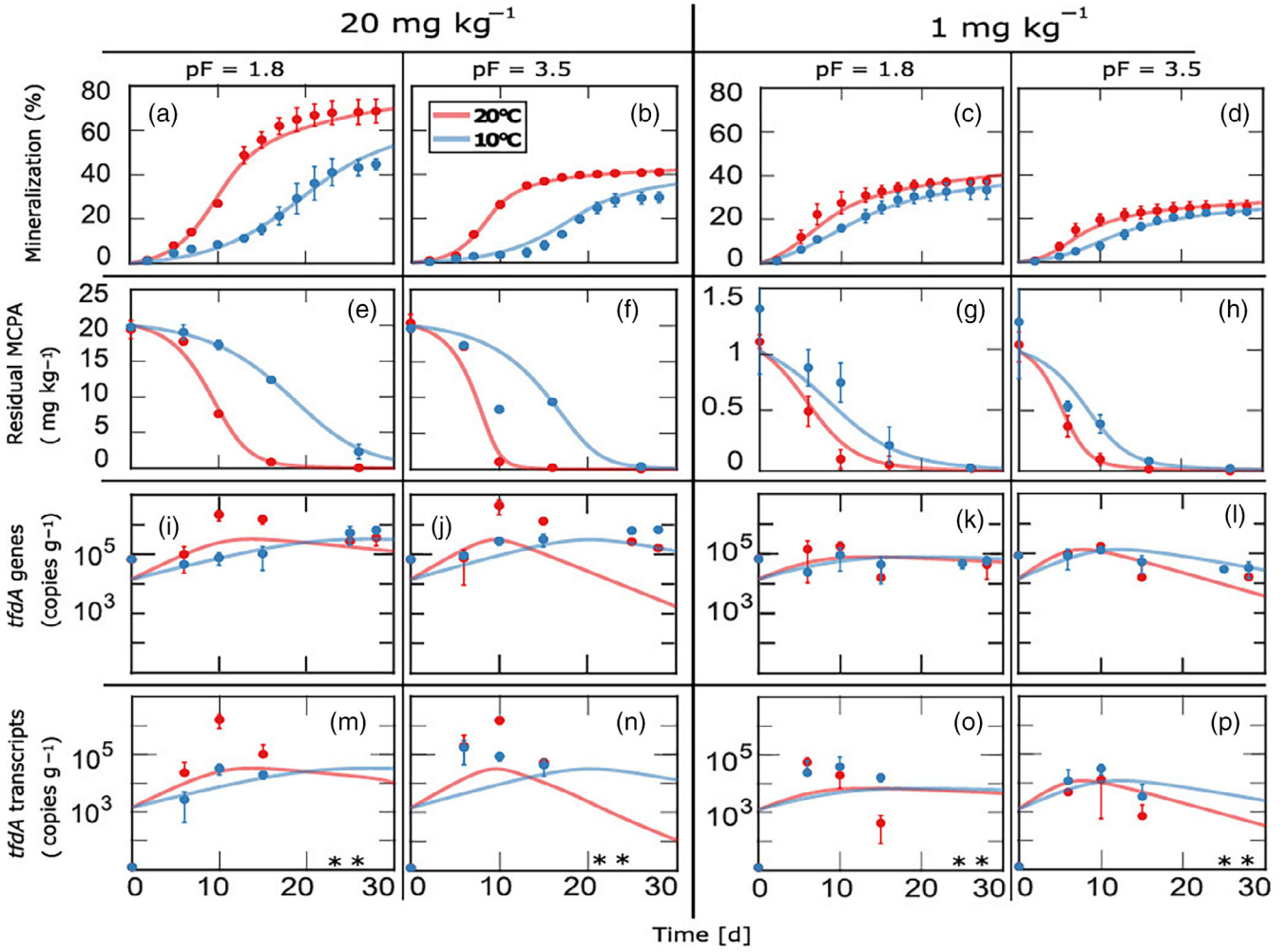

FIGURE 1 Measured (dots) and simulated (lines) of cumulative $^{14}CO_2$ mineralization at two MCPA concentrations as a function of temperature and soil moisture over time (a–d), Residual MCPA expressed as mg kg^{-1} over time (e–h), *tfdA* genes during the MCPA biodegradation experiment expressed as gene copies g^{-1} dw (i–l), *tfdA* transcripts quantities during MCPA degradation expressed as copies g^{-1} dw (m–p). *tfdA* genes and transcripts are expressed at log-scale. Error bars represent standard errors of the mean values for soil triplicates (see Section 2). *tfdA* transcript abundances at days 25 and 28 (* in panels m–p) were below the detection limit and therefore were not included in the model calibration.

3.1.2 | Soil moisture response

As a single factor, reduced soil moisture at pF 3.5 resulted in the strongest decrease in $^{14}CO_2$ mineralization (−16.2% $F_{1,16} = 136$, $p < 0.01$). This effect was most pronounced at the high MCPA concentration ($F_{1,16} = 17.9$, $p < 0.001$), where total mineralization was 21.3% higher at pF 1.8 as compared to pF 3.5 (Figure 1a,b). At the low MCPA concentrations, this increase was only 11.0% (Figure 1c,d). Microbial activity typically decreases with increasing osmotic potential, as demonstrated by Sparling et al. (1989). According to Ilstedt et al. (2000), the reason a reduction in water content also reduces the maximum mineralizable ^{14}C fraction of MCPA is related to substrate diffusion limitation due to the reduced thickness of the water film on soil particles as osmotic potential declines (Papendick & Campbell, 1981). Schroll et al. (2006) determined a water potential for aerobically degradable chemicals of −0.015 MPa, which corresponds to a pF value of about 2.2, slightly below the pF-value of 1.8. Evaluation of MCPA residues (Figure 1e–h) indicated almost complete degradation, especially in the 1 mg kg^{-1} treatment at 20°C, in which MCPA was no longer detectable after 10 to 15 days. Ten percent of the initially applied MCPA remained in the soil only under the treatment combination of 20 mg kg^{-1}, 10°C and pF 1.8. In the treatment combination of pF 3.5 and 20°C, no MCPA could be extracted after 20 days. If the incubation took place at 10°C, MCPA was no longer detectable after 25 days. Similar detection times for MCPA were reported by Baelum et al. (2006), Baelum et al. (2006), Hiller et al. (2009), and Peña et al. (2015).

3.2 | Microbial growth and activity under varying soil conditions during MCPA degradation

Potential of MCPA degradation and microbial activity were measured through *tfdA* gene (Figure 1i–l) and transcript abundances (Figure 1m–p), respectively. The *tfdA* gene abundance responded only to the 20 mg kg^{-1} and 20°C treatments (Figure 1i,j). The abundance of *tfdA* genes reached a maximum 10 days after MCPA application; with significantly higher copy numbers at pF 3.5 ($4.3 \cdot 10^6$ copies g^{-1} dry weight (dw)) than at pF 1.8 ($2.2 \cdot 10^6$ copies g^{-1} dw; day:pF; $F_{1,24} = 16{,}48$, $p < 0.01$). After the peak, a slow decline followed until day 28, after which the initial level of 10^4 copies g^{-1} dw was reached again. The concentration-dependent proliferation of *tfdA*-harbouring microorganisms is consistent with the study by Bælum et al. (2008), which demonstrated a similar increase from $1 \cdot 10^4$ to $3 \cdot 10^6$ copies g^{-1} dw during the degradation of 20 mg kg^{-1} MCPA. Below 20 mg kg^{-1}, *tfdA* DNA remained at a consistently low level, indicating no growth occurred during mineralization (Nicolaisen et al., 2008). The response of *tfdA* transcripts to concentration and temperature mirrored the patterns of *tfdA* gene abundance (concentration:day:temperature; $F_{8,96} = 30.01$, $p < 0.001$), with a clear response to the treatment of 20 mg kg^{-1} MCPA at 20°C. However, soil moisture had no effect on gene transcription ($F_{1,24} = 1.51$, $p = 0.90$). We also observed a correlation between the detected levels of *tfdA* mRNA (Figure 1m–p) and the mineralized pesticide (Figure 1a–d). For example, no *tfdA* mRNA was detected in the control treatments (data not shown), and *tfdA* mRNA was only detected once mineralization of MCPA could be measured. After a lag phase of approximately 5 days, there was a slow increase in $^{14}CO_2$-mineralization accompanied by an increase in *tfdA* mRNA from an average of 10^1 on day 0 to a peak of 10^6 copies g^{-1} dw on day 10. At this time, the inflection point of the sigmoidal $^{14}CO_2$ mineralization curve was attained: i.e., the maximum degradation intensity. Subsequently, $^{14}CO_2$-mineralization decreased again, coinciding with a drop in *tfdA* transcript abundance, which fell below our detection limit (10^3 copies g^{-1} dw) for mRNA quantification at day 28 (Figure 1m,n). Similar results were obtained by Vieublé Gonod (2002) and Bælum et al. (2008), where an initial "lag" period (0–8 days) with minor mineralization indicated limited microbial pesticide turnover. In a second phase characterized by a sharp increase in mineralization (after day eight), Bælum et al. (2008) detected a maximum *tfdA* level of $\sim 10^4$ transcripts per gram soil on day 16, followed by a decline to approximately 10^3 copies on day 24. The observed patterns of *tfdA* gene and transcript dynamics were well captured by gene-based mechanistic model simulation. According to Gözdereliler et al. (2013), different degrader subpopulations are adapted to different MCPA concentrations. Therefore, we allowed the parameters f_1 (conversion factor cell to C), m (maintenance coefficient), and Y_P (yield coefficient) to take different values at 1 and 20. Calibrated parameters (Table S6) suggested populations with bigger cells, higher maintenance demands, and lower yield efficiencies at 20 mg kg^{-1} than at 1 mg kg^{-1}, which is in accordance with Gözdereliler et al. (2013). Additionally, within each concentration level, slightly smaller cells with low maintenance demands and high yield efficiencies might be expected at pF 3.5.

3.3 | CUE dependency on temperature, moisture, and MCPA concentration

We determined CUE_M based on measured ^{14}C incorporation into microbial biomass (Sinsabaugh et al., 2013). Additionally, and taking advantage of our mechanistic gene-centric model, we derived two model-based CUEs – CUE_E and CUE_C. While CUE_M accounts for pesticide-derived C incorporation into the entire microbial community, the two model-based CUEs exclusively consider C utilization by specific pesticide degraders. CUE_M and CUE_E measure the effects of pesticide-C stabilization on C utilization over a longer period, considering the effects of biomass turnover, substrate recycling, and potential cross-feeding (Geyer et al., 2016). CUE_C is calculated from simulated process rates and measures the immediate C utilization after MCPA uptake.

3.3.1 | ^{14}C uptake

The prerequisite for CUE_M assessment is quantification of ^{14}C incorporation into the biomass ($^{14}C_{mic}$). Soil moisture did not affect $^{14}C_{mic}$ (Table S13). In contrast, a temperature reduction to 10°C significantly increased $^{14}C_{mic}$ during the first 5 days after MCPA application by 3 percentage points to 10% ($F_{1,16} = 4.9$, $p < 0.05$), compared to the 20°C treatment. Microbial uptake of MCPA can occur very quickly, according to Nowak et al. (2011), who found a peak in 2,4-D derived ^{13}C after only 2 days. They identified bacteria as the main degraders of 2,4-D in the soil. However, an initial high $^{14}C_{mic}$ is followed by ^{14}C losses, since the ^{14}C is assimilated to form precursor compounds for further biosynthesis or is dissimilated for maintenance respiration (Geyer et al., 2016).

3.3.2 | Community CUE_C

Short-term metabolic reaction of degraders is represented by the CUE_C (Figure S3). On average, CUE_C increased by 0.2 at 1 mg kg^{-1} compared to 20 mg kg^{-1}. The CUE_C in relation to the remaining MCPA concentration reached zero at 1 and pF 1.8 after about 99% of the initially applied MCPA was degraded; this was in contrast to the 20mg kg^{-1} treatment, where this point was reached earlier (90%, Figure S3). These findings indicate a more efficient utilization of MCPA-derived C at low initial concentrations and longer-lasting gross production. Gross production is defined as total pesticide uptake minus pesticide-C, which is mineralized and used for further biosynthesis processes (Geyer et al., 2016). Therefore, in contradiction to the constant metabolic flux analysis of Geyer et al. (2019), in which no change in the biochemical processes was detected during the incubation of different glucose concentrations, we can confirm a decrease in CUE_C for MCPA at 20mg kg^{-1}. Lower CUE_C under higher MCPA concentration is likely attributable to two different fitted values of growth yield parameters for each initial MCPA concentration (Table S6). This finding supports the inherent model assumption made in accordance with Gözdereliler et al. (2013) that two subpopulations of pesticide degraders with different physiologies trigger concentration-dependent shifts in pesticide-C metabolism. Metabolic regulations leading to increased nutrient-mobilizing extracellular enzymes or C-wasting respiratory mechanisms under nutrient limitations could also be responsible for lower CUE_C (Manzoni et al., 2017). However, these processes can be ruled out in fertilized soils, because in these soils nutrient limitations are not expected.

3.3.3 | Environmental CUE_M and simulated CUE_E

Short-term differences in CUE_C should affect the long-term fate of the MCPA-C, as measured by CUE_M and CUE_E. CUE_M was significantly higher during the MCPA degradation at 20mg kg^{-1} compared to 1mg kg^{-1} (+0.06; $F_{1,16} = 5.8$, $p < 0.05$) during the first 15 days (Figure 2a–d). CUE_M can only be statistically evaluated by comparison at each time point. However, comparing CUE_M over time is misleading, as different states of degradation dynamics are being compared. To eliminate this deviation, CUE_E was considered as a function of the relative decrease in MCPA concentration (Figure 2e–h). The simulated CUE_E is about 0.2 higher at low concentrations than at high concentrations, indicating greater C stabilization at the ecosystem level at low concentrations. For CUE_M, this effect was only evident at the end of the incubation ($CUE = 0.21$; $F_{1,16} = 4.3$, $p = 0.05$).

We observed an increase in CUE_M with decreasing temperature (Figure 2a–d), which also has previously been reported (Dacal et al., 2021; Domeignoz-Horta et al., 2020; Frey et al., 2013), and is associated with higher growth efficiencies (Domeignoz-Horta et al., 2020; Pold et al., 2020) and lower energy costs to maintain existing biomass (Gözdereliler et al., 2013; Sinsabaugh et al., 2013). An additional temperature effect is that increased microbial activity at 20°C leads to increased MCPA turnover especially at 20 mg kg^{-1}, which is in agreement with the Arrhenius equation (Laidler, 1984). The substrate concentration was therefore present longer at 10°C and as a result, maintained a higher CUE_M for a longer time (Figure 2e–h). The simulated CUEs did not indicate the temperature effect (Figure 2e–h), because the model assumptions for CUE_E and CUE_C assign the same temperature sensitivity to microbial growth, maintenance and turnover (see Equation 2, 4, 5, 6 and 7 in the Appendix S1: Section 1.7.1).

In addition to concentration and temperature, CUE_M was increased by the reduction in soil moisture (+ 0.15; $F_{1,16} = 40.3$, $p < 0.01$), especially at the first time point (fifth day). Similarly, CUE_E and CUE_C were 0.25 higher at pF 3.5 (Figure 2). Consistent with this finding of our study, Jones et al. (2018) found an upward trend in microbial CUE under the following aridity levels: hyper-arid > arid > semi-arid, with the subsequent finding that even under hyper-dry conditions, very low microbial activity and C turnover occurred with altered C allocation. The reason given was reduced catalytic activity related to a decline in motility of organisms and enzymes across a water film that loses thickness as drought increases. However, this is not a common finding, as many studies (Ågren et al., 2001; Allison et al., 2010) have shown that microbial *CUE* in soil can decline with lower water content and substrate availability. In addition to the reduced catalytic activity, the efficient utilization of MCPA by the specific microorganisms could also lead to this increased *CUE* under dry soil conditions, setting it apart from the turnover of soil organic matter by the entire soil microbial community. Interestingly, increased *CUE* with reduced temperature and soil moisture was not accompanied by any response of *tfdA* transcript and gene copy numbers in our study. This imbalance may be explained by the fact that microbial use of the substrate is more complex than simple conversion to biomass (Schimel & Schaeffer, 2012). Rather, bacterial degraders synthesize a variety of products, e.g., to maintain basic functions, such as extracellular enzymes, extracellular polysaccharides, cell wall polymers, but also stress response compounds, such as osmolytes, to survive

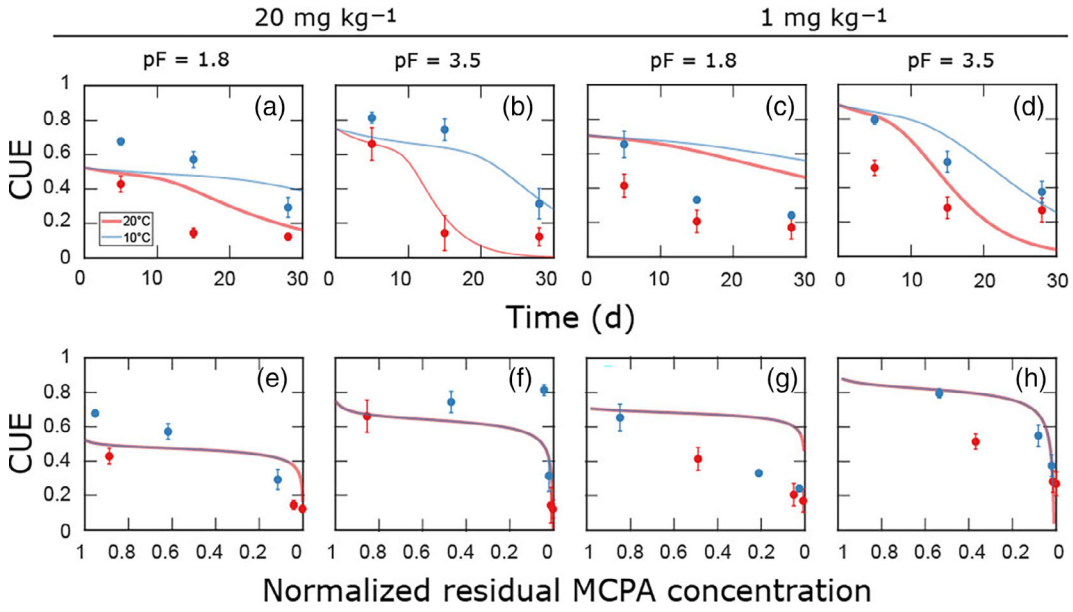

FIGURE 2 *CUE* vs. time (d) showed in panels a–d, and *CUE* vs normalized residual MCPA concentration in soil showed in panels e–h. CUE_M (Equation 11) is presented as points and CUE_E (Equation 12) as lines. Note that the CUE_M were not used for model calibration (see Section 2).

TABLE 2 Half-life DT_{50RES} derived from the residual MCPA concentration in soils and DT_{50MIN} derived from mineralization kinetics as a function of soil moisture, concentration, and temperature.

	DT_{50RES}						DT_{50MIN}					
	pF 1.8			**pF 3.5**			**pF 1.8**			**pF 3.5**		
	10°C	**20°C**	**10°C/20°C**	**10°C**	**20°C**	**10°C/20°C**	**10°C**	**20°C**	**10°C/20°C**	**10°C**	**20°C**	**10°C/20°C**
20 mg kg^{-1}	18.4	9.3	2.0	15.6	7.4	2.1	18.5	9.9	**1.9**	17.6	8.8	**2.0**
1 mg kg^{-1}	9.6	6.5	1.5	8.5	5.4	**1.6**	10.3	6.7	**1.5**	12.2	6.3	**1.9**

under dry conditions (Schimel et al., 2007). This formation of stress compounds could explain a slight increase in C use efficiencies during MCPA degradation under drier conditions compared to the near-optimal water content at pF 1.8.

3.3.4 | Differences in mineralization and dynamics of actual MCPA decline

Differences in MCPA degradation were also reflected in DT_{50}-values, describing the time required to mineralize 50% of the applied MCPA (Table 2). We determined two different DT_{50} values: (i) a DT_{50MIN} derived from mineralization kinetics, typically calculated in dissipation experiments of pesticides, and (ii) a DT_{50RES} derived from residual MCPA concentration. Under limiting conditions, we observed longer DT_{50RES} and DT_{50MIN}-values, with temperature exerting a stronger influence than soil moisture. Based on mineralization kinetics, we found that the residence time of MCPA increased by a factor of 1.9 when soil moisture and temperature were reduced at 1 mg kg^{-1} (Table 2). The DT_{50RES} value indicated that the residence time increased only by a factor of 1.6. This deviation in estimated residence time, could be due to altered temperature- and soil moisture-dependent C allocation, which is supported by the increased *CUE* under the treatment combination pF 3.5, 10°C, and 1 mg kg^{-1}. Consequently, the determination of degradation dynamics based on ^{14}C curves becomes unreliable. Under limiting conditions, mineralization was no longer proportional to the dynamics of the actual degradation processes (Table 2).

Compared to the concentration of 1 mg kg^{-1}, the effect of a temperature reduction at 20 mg kg^{-1} was independent of both soil moisture and the DT_{50} approach, increasing half-life times by a factor of ~2 (Table 2). In this case, degradation was initially limited by the number of microorganisms, in contrast to degradation at 1 mg kg^{-1}, where degradation potential was provided by

the autochthonous microbial abundance; here, rapid first-order degradation could be initiated immediately (Baelum et al., 2006; Wirsching et al., 2020). According to Babey et al. (2017), degradation of 2,4-D is most efficient when the ratio of degraders to instantaneous pesticide concentrations favours degraders. This was the case for the treatment at 20°C and high initial pesticide concentration after a relatively low mineralization was observed in the first phase of the experiment (0–5 days). In the absence of growth at 10°C, as indicated by the lack of any increase in *tfdA* copy numbers, DT_{50MIN} and DT_{50RES} values were significantly higher, indicating slower degradation.

4 | CONCLUSION

Our results partially contradict previous findings (Bouseba et al., 2009; Castillo & Torstensson, 2007; Cattaneo et al., 1997; Parker & Doxtader, 1983) that claim a decrease in temperature and soil moisture during MCPA biodegradation is always accompanied by a significant increase in half-life time. The extent to which the residence time of MCPA was affected by a change in temperature and soil moisture depended solely on initial concentration and associated degradation dynamics. This study demonstrates that ^{14}C incorporation is not necessarily proportional to mineralization, confirming the hypothesis that, under limiting conditions, assimilation is enhanced to support anabolic processes. C dissimilation including non-growth maintenance (Geyer et al., 2016), increased with rising temperatures, as energy costs became more important regulators of motility or molecular turnover of proteins (Russell & Cook, 1995). As a result, the MCPA-derived C will be used more efficiently by microorganisms at low temperatures and reduced soil moisture. Under these circumstances, estimating DT_{50}-values from cumulative mineralization will likely lead to a systematic underestimation of pesticide degradation.

We expect that our findings for MCPA are valid for other pesticides with similar degradation pathways such as 2,4-Dichlorophenol (2,4-D) or 4-Chloro-2-methylphenol (mecoprop), although pesticides with other properties may behave differently. However, the temperature sensitivity of pesticide degradation can be strongly influenced by the sorption affinity of the pesticide. Under conditions of lower availability of highly sorptive pesticides such as glyphosate, the measured or apparent temperature sensitivity and *CUE* fluctuations may be lower than observed for MCPA degradation. How CUE responds during pesticide degradation under anaerobic conditions would be another interesting point to investigate. Further research is needed to determine the validity of the proposed mechanisms for pesticides with different properties.

AUTHOR CONTRIBUTIONS

Johannes Wirsching: Conceptualization; investigation; writing – original draft; methodology; validation; visualization; software; formal analysis; data curation. **Luciana Chavez Rodriguez:** Writing – original draft; validation; visualization; methodology; software; formal analysis; investigation. **Franziska Ditterich:** Methodology; data curation; formal analysis; writing – review and editing. **Holger Pagel:** Conceptualization; methodology; supervision; writing – review and editing; validation; software. **Rushan He:** Writing – review and editing; formal analysis. **Marie Uksa:** Writing – review and editing; methodology; conceptualization. **Christian Zwiener:** Writing – review and editing; methodology. **Ellen Kandeler:** Writing – review and editing; funding acquisition; methodology; resources. **Christian Poll:** Project administration; supervision; writing – review and editing; funding acquisition.

ACKNOWLEDGEMENTS

The authors acknowledge support by the State of Baden-Württemberg through bwHPC. We would like to thank Stephanie Nowak from the Environmental Analytical Chemistry Department in Tübingen for measuring the MCPA concentrations and Kathleen Regan for the English corrections. Open Access funding enabled and organized by Projekt DEAL.

FUNDING INFORMATION

This study was financially supported by the German Research Foundation (DFG) within the Research Training Group "Integrated Hydrosystem modeling" (RTG 1829) and the Collaborative Research Center 1253 CAMPOS (DFG Grant Agreement SFB 1253/12017) as well as by the Ellrichshausen Foundation.

CONFLICT OF INTEREST STATEMENT

The authors have no conflicts of interest related to this article.

DATA AVAILABILITY STATEMENT

The data that support the findings of this study are openly available in Luciana-cloud/allocation_MCPA: allocation_pesticide at https://doi.org/10.5281/zenodo.5081655.

REFERENCES

Ågren, G. I., Bosatta, E., & Magill, A. H. (2001). Combining theory and experiment to understand effects of inorganic nitrogen on litter decomposition. *Oecologia*, *128*, 94–98.

Allison, S. D., Wallenstein, M. D., & Bradford, M. A. (2010). Soil-carbon response to warming dependent on microbial physiology. *Nature Geoscience*, *3*(5), 336–340. https://doi.org/10.1038/ngeo846

Audus, L. J. (1952). The decomposition of 2:4-dichlorophenoxyacetic acid and 2-methyl-4-chlorophenoxyacetic acid in the soil. *Journal of the Science of Food and Agriculture*, *3*(6), 268–274. https://doi.org/10.1002/jsfa.2740030607

Babey, T., Vieublé-gonod, L., Rapaport, A., Pinheiro, M., Garnier, P., & Dreuzy, D., Jr. (2017). Spatiotemporal simulations of 2,4-Dpesticide degradation by microorganisms in 3D soil-core experiments. *Ecological Modelling*, *344*, 48–61. https://doi.org/10.1016/j.ecolmodel.2016.11.006

Baelum, J., Henriksen, T., Hansen, H. C. B., & Jacobsen, C. S. (2006). Degradation of 4-chloro-2-methylphenoxyacetic acid in top- and subsoil is quantitatively linked to the class III tfdA gene. *Applied and Environmental Microbiology*, *72*(2), 1476–1486.

Bælum, J., Nicolaisen, M. H., Holben, W. E., Strobel, B. W., Sørensen, J., & Jacobsen, C. S. (2008). Direct analysis of tfdA gene expression by indigenous bacteria in phenoxy acid amended agricultural soil. *ISME Journal*, *2*(6), 677–687.

Bouseba, B., Zertal, A., Beguet, J., Rouard, N., Devers, M., Martin, C., & Martin-Laurent, F. (2009). Evidence for 2,4-D mineralisation in mediterranean soils. *Pest Management Science*, *65*(9), 1021–1029.

Castillo, M. P., & Torstensson, L. (2007). Effect of biobed composition, moisture, and temperature on the degradation of pesticides. *Journal of Agricultural and Food Chemistry*, *55*(14), 5725–5733.

Cattaneo, M. V., Masson, C., & Greer, C. W. (1997). The influence of moisture onmicrobial transport, survival and 2,4-D biodegradation with a genetically marked Burkholderia cepacia in unsaturated soil columns. *Biodegradation*, *8*(2), 87–96. https://doi.org/10.1023/A:1008236401342TS-CrossRef

Chavez Rodriguez, L., Ingalls, B., Schwarz, E., Streck, T., Uksa, M., & Pagel, H. (2020). Gene-centric model approaches for accurate prediction of pesticide biodegradation in soils. *Environmental Science & Technology*, *54*(21), 13638–13650.

Choi, J. S., Fermanian, T. W., Wehner, D. J., & Spomer, L. A. (1988). Effect of temperature, moisture, and soil texture on DCPA degradation. *Agronomy Journal*, *80*(1), 108–113.

Dacal, M., Delgado-Baquerizo, M., Barquero, J., Berhe, A. A., Gallardo, A., Maestre, F. T., & Garcia-Palacios, P. (2021). Temperature increases soil res piration across ecosystem types and soil development, but soil properties determine the magnitude of this effect. *Ecosystems*, *25*, 184–198.

Davidson, E. A., & Janssens, I. A. (2006). Temperature sensitivity of soil carbon decomposition and feedbacks to climate change. *Nature*, *440*(7081), 165–173.

Ditterich, F., Poll, C., Pagel, H., Babin, D., Smalla, K., Horn, M. A., Streck, T., & Kandeler, E. (2013). Succession of bacterial and fungal 4-chloro-2- methylphenoxyacetic acid degraders at the soil – Litter interface. *FEMS Microbiology Ecology*, *86*, 85–100.

Domeignoz-Horta, L. A., Pold, G., Liu, X. J. A., Frey, S. D., Melillo, J. M., & DeAngelis, K. M. (2020). Microbial diversity drives carbon use efficiency in a model soil. *Nature Communications*, *11*(1), 3684.

Dörfler, U., Haala, R., Matthies, M., & Scheunert, I. (1996). Mineralization kinetics of chemicals in soils in relation to environmental conditions. *Ecotoxicology and Environmental Safety*, *34*(3), 216–222. https://doi.org/10.1006/eesa.1996.0066

Duo-Sen, L., & Shui-Ming, Z. (1987). Kinetic model for degradative processes of pesticides in soil. *Ecological Modelling*, *37*(3), 131–138.

Fomsgaard, I. S., & Kristensen, K. (1999). Influence of microbial activity, organic carbon content, soil texture and soil depth on mineralisation rates of low concentrations of 14C-mecoprop—Development of a predictive model. *Ecological Modelling*, *122*(1–2), 45–68.

Fredslund, L., Vinther, F. P., Brinch, U. C., Elsgaard, L., Rosenberg, P., & Jacobsen, C. S. (2008). Spatial variation in 2-Methyl-4- chlorophenoxyacetic acid mineralization and sorption in a Sandy soil at field level. *Journal of Environmental Quality*, *37*(5), 1918–1928.

Frey, S. D., Lee, J., Melillo, J. M., & Six, J. (2013). The temperature response of soil microbial efficiency and its feedback to climate. *Nature Climate Change*, *3*(4), 395–398.

Geyer, K. M., Dijkstra, P., Sinsabaugh, R., & Frey, S. D. (2019). Clarifying the interpretation of carbon use efficiency in soil through methods comparison. *Soil Biology and Biochemistry*, *128*, 79–88.

Geyer, K. M., Kyker-Snowman, E., Grandy, A. S., & Frey, S. D. (2016). Microbial carbon use efficiency: Accounting for population, community, and ecosystem-scale controls over the fate of metabolized organic matter. *Biogeochemistry*, *127*(2), 173–188.

Gözdereliler, E., Boon, N., Aamand, J., De Roy, K., Granitsiotis, M. S., Albrechtsen, H. J., et al. (2013). Comparing metabolic functionalities, community structures, and dynamics of herbicide-degrading communities cultivated with different substrate concentrations. *Applied and Environmental Microbiology*, *79*(1), 367–375.

Griffin, D. M. (1969). Soil water in the ecology of fungi. *Annual Review of Phytopathology*, *7*, 289–310.

Griffin, D. M. (1981). Water potential as a selective factor in the microbial ecology of soils. In J. F. Parr, W. R. Gardner, & L. F. Elliott (Eds.), *Water potential relations in soil microbiology* SSSA special publications TS – CrossRef, [S.L.] (pp. 141–151). SSSA.

Helweg, A. (1987). Degradation and adsorption of 14C-MCPA in soil—Influence of concentration, temperature and moisture content on degradation. *Weed Research*, *27*(4), 287–296. https://doi.org/10.1111/j.1365-3180.1987.tb00765.x

Helweg, A. (1993). Degradation and adsorption of 14C-mecoprop (MCPP) in surface soils and in subsoil. Influence of temperature, moisture content, sterilization and concentration on degradation. *Science of the Total Environment*, *132*(2–3), 229–241.

Helweg, A., Fomsgaard, I. S., Reffstrup, T. K., & Srensen, H. (1998). Degradation of Mecoprop and Isoproturon in soil influence of initial concentration. *International Journal of Environmental Analytical Chemistry*, *70*(1–4), 133–148.

Hiller, E., Bartaľ, M., Milička, J., & Čerňanský, S. (2009). Environmental fate of the herbicide MCPA in two soils as affected by the presence of wheat ash. *Water, Air, and Soil Pollution*, *197*(1–4), 395–402.

Ilstedt, U., Nordgren, A., & Malmer, A. (2000). Optimum soil water for soil respiration before and after amendment with glucose in humid tropical acrisols and a boreal mor layer. *Soil Biology and Biochemistry*, *32*(11), 1591–1599.

Ingalls, B. (2008). Sensitivity analysis: From model parameters to system behaviour local sensitivity analysis: Derivation. *Essays in Biochemistry*, *45*, 177–193.

Jones, D. L., Olivera-Ardid, S., Klumpp, E., Knief, C., Hill, P. W., Lehndorff, E., & Bol, R. (2018). Moisture activation and carbon use efficiency of soil microbial communities along an aridity gradient in the Atacama Desert. *Soil Biology and Biochemistry*, *117*, 68–71.

Jury, W. A., Spencer, W. F., & Farmer, W. J. (1987). Behavior assessment model for trace organics in soil: I. Model description. *Journal of Environmental Quality*, *16*(4), 448.

Karanasios, E., Karpouzas, D. G., & Tsiropoulos, N. G. (2012). Key parameters and practices controlling pesticide degradation efficiency of biobed substrates. *Journal of Environmental Science and Health, Part B*, *47*(6), 589–598.

Kozak, M., & Piepho, H. P. (2018). What's normal anyway? Residual plots are more telling than significance tests when checking ANOVA assumptions. *Journal of Agronomy and Crop Science*, *204*(1), 86–98.

Laidler, K. J. (1984). The development of the Arrhenius equation. *Journal of Chemical Education*, *61*(6), 494.

Lenth, R., Buerkner, P., Herve, M., Love, J., Riebl, H., & Singmann, H. (2020). Emmeans. https://github.com/rvlenth/emmeansM4-Citavi

Leveau, J. H. J., König, F., Füchslin, H., Werlen, C., & Van Der Meer, J. R. (1999). Dynamics of multigene expression during catabolic adaptation of Ralstonia eutropha JMP134 (pJP4) to the herbicide 2,4-dichlorophenoxyacetate. *Molecular Microbiology*, *33*(2), 396–406.

Malwade, A., Nguyen, A., Sadat-Mousavi, P., & Ingalls, B. P. (2017). Predictive modeling of a batch filter mating process. *Frontiers in Microbiology*, *8*, 1–11.

Manzoni, S., Čapek, P., Mooshammer, M., Lindahl, B. D., Richter, A., & Šantrůčková, H. (2017). Optimal metabolic regulation along resource stoichiometry gradients. *Ecology Letters*, *20*(9), 1182–1191.

Manzoni, S., Čapek, P., Porada, P., Thurner, M., Winterdahl, M., Beer, C., Brüchert, V., Frouz, J., Herrmann, A. M., Lindahl, B. D., Lyon, S. W., Šantrůčková, H., Vico, G., & Way, D. (2018). Reviews and syntheses: Carbon use efficiency from organisms to ecosystems–definitions, theories, and empirical evidence. *Biogeosciences*, *15*(19), 5929–5949. https://doi.org/10.5194/bg-15-5929-2018

Manzoni, S., Schaeffer, S. M., Katul, G., Porporato, A., & Schimel, J. P. (2014). A theoretical analysis of microbial ecophysiological and diffusion limitations to carbon cycling in drying soils. *Soil Biology and Biochemistry*, *73*, 69–83.

Manzoni, S., Schimel, J. P., & Porporato, A. (2012). Responses of soil microbial communities to water stress: Results from a meta analysis. *Ecology*, *93*(4), 930–938.

Moyano, F. E., Manzoni, S., & Chenu, C. (2013). Responses of soil heterotrophic respiration to moisture availability: An exploration of processes and models. *Soil Biology and Biochemistry*, *59*, 72–85.

Muskus, A. M., Krauss, M., Miltner, A., Hamer, U., & Nowak, K. M. (2019). Effect of temperature, pH and total organic carbon variations on microbial turnover of 13C315N-glyphosate in agricultural soil. *Science of the Total Environment*, *658*, 697–707.

Muskus, A. M., Krauss, M., Miltner, A., Hamer, U., & Nowak, K. M. (2020). Degradation of glyphosate in a Colombian soil is influenced by temperature, total organic carbon content and pH. *Environmental Pollution*, *259*, 113767.

Nicolaisen, M. H., Bælum, J., Jacobsen, C. S., & Sørensen, J. (2008). Transcription dynamics of the functional tfdA gene during MCPA herbicide degradation by Cupriavidus necator AEO106 (pRO101) in agricultural soil. *Environmental Microbiology*, *10*(3), 571–579.

Nowak, K. M., Miltner, A., Gehre, M., Schäffer, A., & Kästner, M. (2011). Formation and fate of bound residues from microbial biomass during 2,4-D degradation in soil. *Environmental Science & Technology*, *45*(3), 999–1006.

Nowak, K. M., Miltner, A., Poll, C., Kandeler, E., Streck, T., & Pagel, H. (2020). Plant litter enhances degradation of the herbicide MCPA and increases formation of biogenic non-extractable residues in soil. *Environment International*, *142*, 105867.

Oh, K. H., Ahn, S. K., Yoon, K. H., & Kim, Y. S. (1995). Biodegradation of the phenoxy herbicide MCPA by microbial consortia isolated from a rice field. *Bulletin of Environmental Contamination and Toxicology*, *55*(4), 539–545.

Pagel, H., Poll, C., Ingwersen, J., Kandeler, E., & Streck, T. (2016). Modeling coupled pesticide degradation and organic matter turnover: From gene abundance to process rates. *Soil Biology and Biochemistry*, *103*, 349–364.

Papendick, R. I., & Campbell, G. S. (1981). Theory and measurement of water potential.

Parker, L. W., & Doxtader, K. G. (1983). Kinetics of the microbial degradation of 2,4-D in soil. *Journal of Environmental Quality*, *12*(4), 553–558.

Parr, J. F., Gardner, W. R., & Elliott, L. F. (1981). In J. F. Parr, W. R. Gardner, & L. F. Elliott (Eds.), *Water potential relations in soil microbiology*. SSSA.

Patzko, T. (2009). Degradation of MCPA in soil horizons of polish agricultural soils. *Polish Journal of Environmental Studies*, *18*, 1083–1091.

Peña, D., López-Piñeiro, A., Albarrán, Á., Becerra, D., & Sánchez-Llerena, J. (2015). Environmental fate of the herbicide MCPA in Agri cultural soils amended with fresh and aged de-oiled two-phase olive mill waste. *Environmental Science and Pollution Research*, *22*(18), 13915–13925.

Pinheiro, J., Bates, D., DebRoy, S., & Sarkar, D. (2020). Linear and nonlinear mixed effects models. https://cran.r-project.org/package=nlme

Pold, G., Domeignoz-Horta, L. A., Morrison, E. W., Frey, S. D., Sistla, S. A., & DeAngelis, K. M. (2020). Carbon use efficiency and its temperature sensitivity covary in soil bacteria. *MBio*, *11*(1), e02293–19.

Poll, C., Pagel, H., Devers-Lamrani, M., Martin-Laurent, F., Ingwersen, J., Streck, T., & Kandeler, E. (2010). Regulation of bacterial and fungal MCPA degradation at the soil–litter interface. *Soil Biology and Biochemistry*, *42*(10), 1879–1887.

Russell, J. B., & Cook, G. M. (1995). Energetics of bacterial growth: Balance of anabolic and catabolic reactions. *Microbiological Reviews*, *59*(1), 48–62.

Schimel, J., Balser, T. C., & Wallenstein, M. (2007). Microbial stress-response physiology and its implications for ecosystem function. *Ecology*, *88*(6), 1386–1394.

Schimel, J. P., & Schaeffer, S. M. (2012). Microbial control over carbon cycling in soil. *Frontiers in Microbiology*, *3*, 348.

Schoen, S., & Winterlin, W. (1987). The effects of various soil factors and amendments on the degradation of pesticide mixtures. *Journal of Environmental Science and Health, Part B*, *22*(3), 347–377.

Schroll, R., Becher, H. H., Dörfler, U., Gayler, S., Grundmann, S., Hartmann, H. P., & Ruoss, J. (2006). Quantifying the effect of soil moisture on the aerobic microbial mineralization of selected pesticides in different soils. *Environmental Science & Technology*, *40*(10), 3305–3312.

Schwarz, E., Khurana, S., Chakrawal, A., Chavez Rodriguez, L., Wirsching, J., Streck, T., Manzoni, S., Thullner, M., & Pagel, H. (2022). Spatial control of microbial pesticide degradation in soil: A model-based scenario analysis. *Environmental Science & Technology*, *56*(20), 14427–14438.

Sierra, C. A., Trumbore, S. E., Davidson, E. A., Vicca, S., & Janssens, I. (2015). Sensitivity of decomposition rates of soil organic matter with respect to simultaneous changes in temperature and moisture. *Journal of Advances in Modeling Earth Systems*, *7*(1), 335–356.

Silva, V., Mol, H. G. J., Zomer, P., Tienstra, M., Ritsema, C. J., & Geissen, V. (2019). Pesticide residues in European agricultural soils – A hidden reality unfolded. *Science of the Total Environment*, *653*, 1532–1545.

Sinsabaugh, R. L., Manzoni, S., Moorhead, D. L., & Richter, A. (2013). Carbon use efficiency of microbial communities. *Ecology Letters*, *16*(7), 930–939.

Sparling, G. P., West, A. W., & Reynolds, J. (1989). Influence of soil moisture regime on the respiration response of soils subjected to osmotic stress. *Soil Research*, *27*(1), 161–168.

Thirunarayanan, K., Zimdahl, R. L., & Smika, D. E. (1985). Chlorsulfuron adsorption and degradation in soil. *Weed Science*, *33*(4), 558–563.

Vance, E. D., Brookes, P. C., & Jenkinson, D. S. (1987). An extraction method for measuring soil microbial biomass C. *Soil Biology and Biochemistry*, *19*(6), 703–707.

Vieublé Gonod, L. (2002). Variabilité spatiale de la minéralisation de substrats carbonés (2,4-D, leucine, lysine) dans la matrice solide du sol. Theses, Université Claude Bernard Lyon 1.

Wirsching, J., Pagel, H., Ditterich, F., Uksa, M., Werneburg, M., Zwiener, C., Berner, D., Kandeler, E., & Poll, C. (2020). Biodegradation of pesticides at the limit: Kinetics and microbial substrate use at low concentrations. *Frontiers in Microbiology*, *11*, 1476.

Yao, K. Z., Shaw, B. M., Kou, B., Mcauley, K. B., & Bacon, D. W. (2003). Modeling ethylene/butene copolymerization with multi-site catalysts: Parameter estimability and experimental design. *Polymer Reaction Engineering*, *11*(3), 563–588.

Zeglin, L. H., Bottomley, P. J., Jumpponen, A., Rice, C. W., Arango, M., Lindsley, A., McGowan, A., Mfombep, P., & Myrold, D. D. (2013). Altered precipitation regime affects the function and composition of soil microbial communities on multiple time scales. *Ecology*, *94*(10), 2334–2345.

Zi, Z. (2011). Sensitivity analysis approaches applied to systems biology models. *IET Systems Biology*, *5*(6), 336–346.

SUPPORTING INFORMATION

Additional supporting information can be found online in the Supporting Information section at the end of this article.

How to cite this article: Wirsching, J., Rodriguez, L. C., Ditterich, F., Pagel, H., He, R., Uksa, M., Zwiener, C., Kandeler, E., & Poll, C. (2023). Temperature and soil moisture change microbial allocation of pesticide-derived carbon. *European Journal of Soil Science*, *74*(5), e13417. https://doi.org/10.1111/ejss.13417